2010 NSF/DOE Partnership on Thermoelectric Devices for Vehicle Applications

High-Performance Thermoelectric Devices Based on Abundant Silicide Materials for Vehicle Waste Heat Recovery

Investigators:

Li Shi, John Goodenough, Matt Hall, Jianshi Zhou

Department of Mechanical Engineering & Texas Materials Institute

University of Texas at Austin

&

Song Jin

Department of Chemistry

University of Wisconsin-Madison

Participating Students:

Chad Baker, Xi Chen, Arden Moore, Annie Weathers (Texas)

Jeremy Higgins, Ankit Pokhrel (Wisconsin)

Collaboration:

Hsin Wang, Oak Ridge National Lab

THE UNIVERSITY OF TEXAS AT AUSTIN

WHAT STARTS HERE CHANGES THE WORLD

THE UNIVERSITY of WISCONSIN MADISON

Overview of Research

Objectives:

a) To increase the *ZT* of abundant silicides to a level competitive with the state of the art found in materials containing much more scarce and expensive elements

b) To enhance the thermal management system performance for silicide TE devices installed in a diesel engine

Tasks:

a) Investigate methods for scalable synthesis and position-dependant doping of bulk nanostructured silicides

b) Explore silicide and alloy interface materials with low contact resistance and improved thermomechanical compliance

c) Characterize the TE properties of silicides at temperatures between 300 and 900 K

d) Develop computation models to guide the heat exchanger design and the placement of the TE elements of spatially varied TE properties

e) Test silicide TE waste heat recovery devices in a 6.7 liter Cummins diesel engine

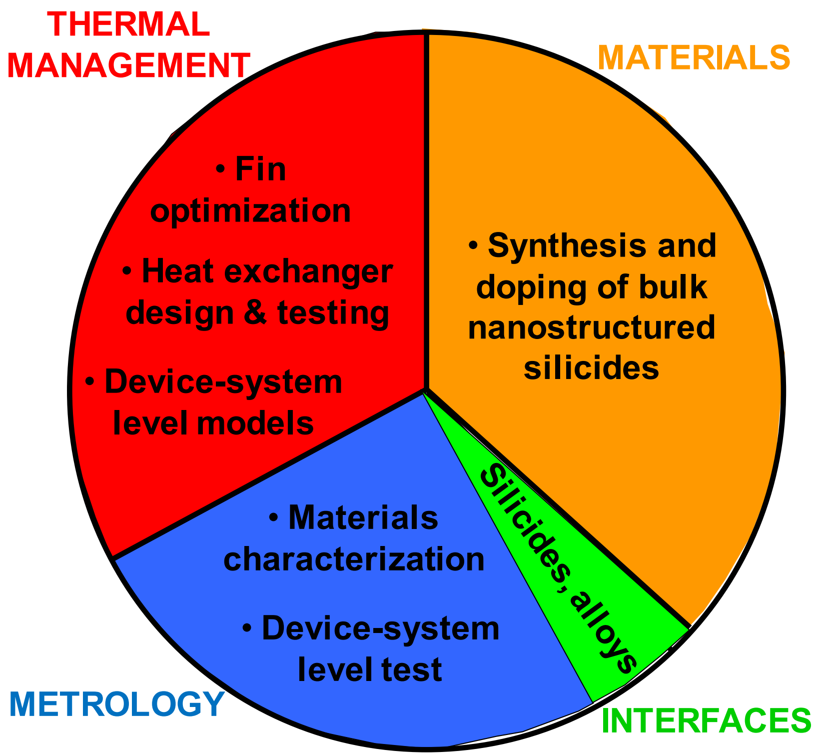

ZT of Bulk Thermoelectric Materials

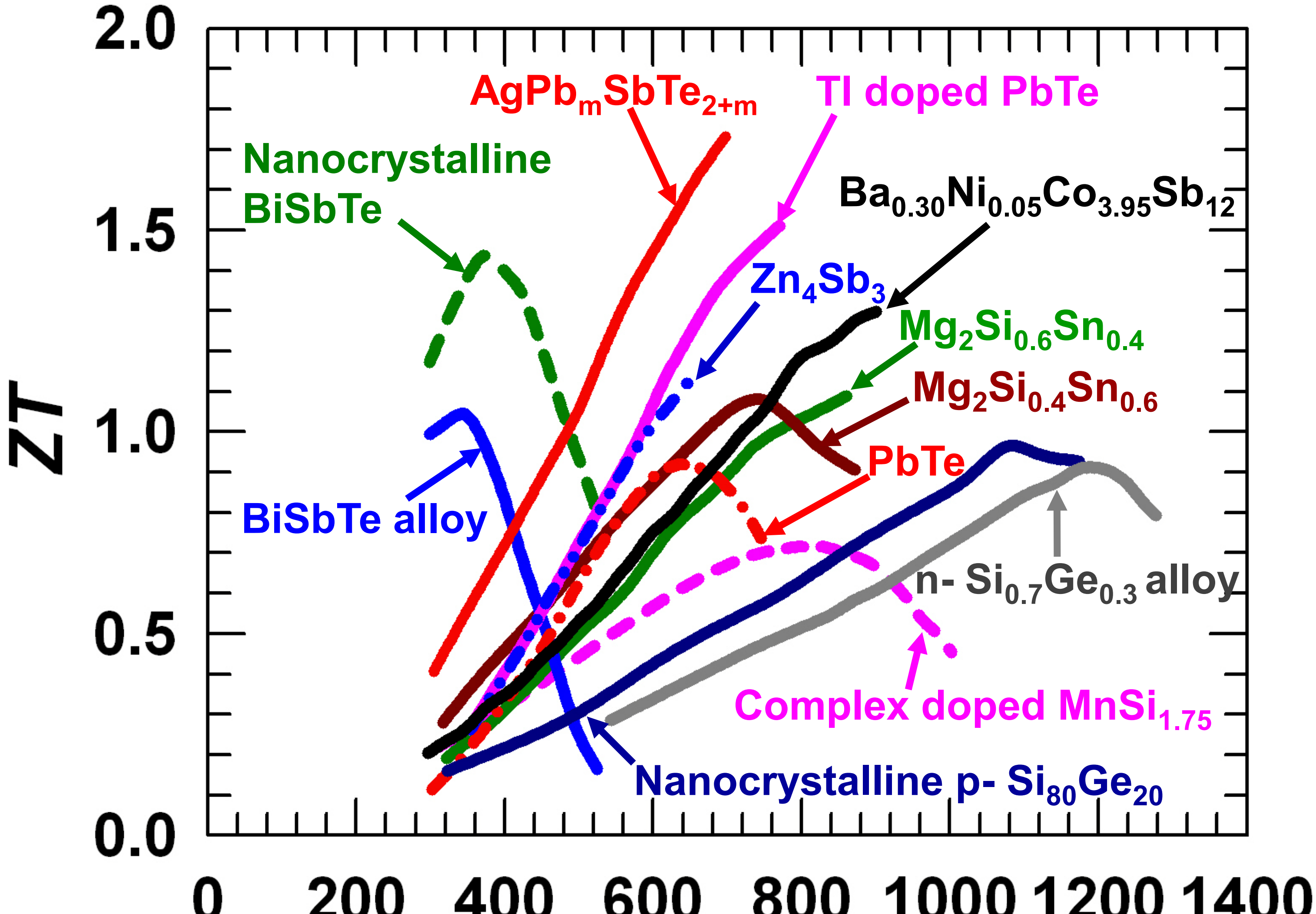

[redacted]

Index of Abundance of Elements

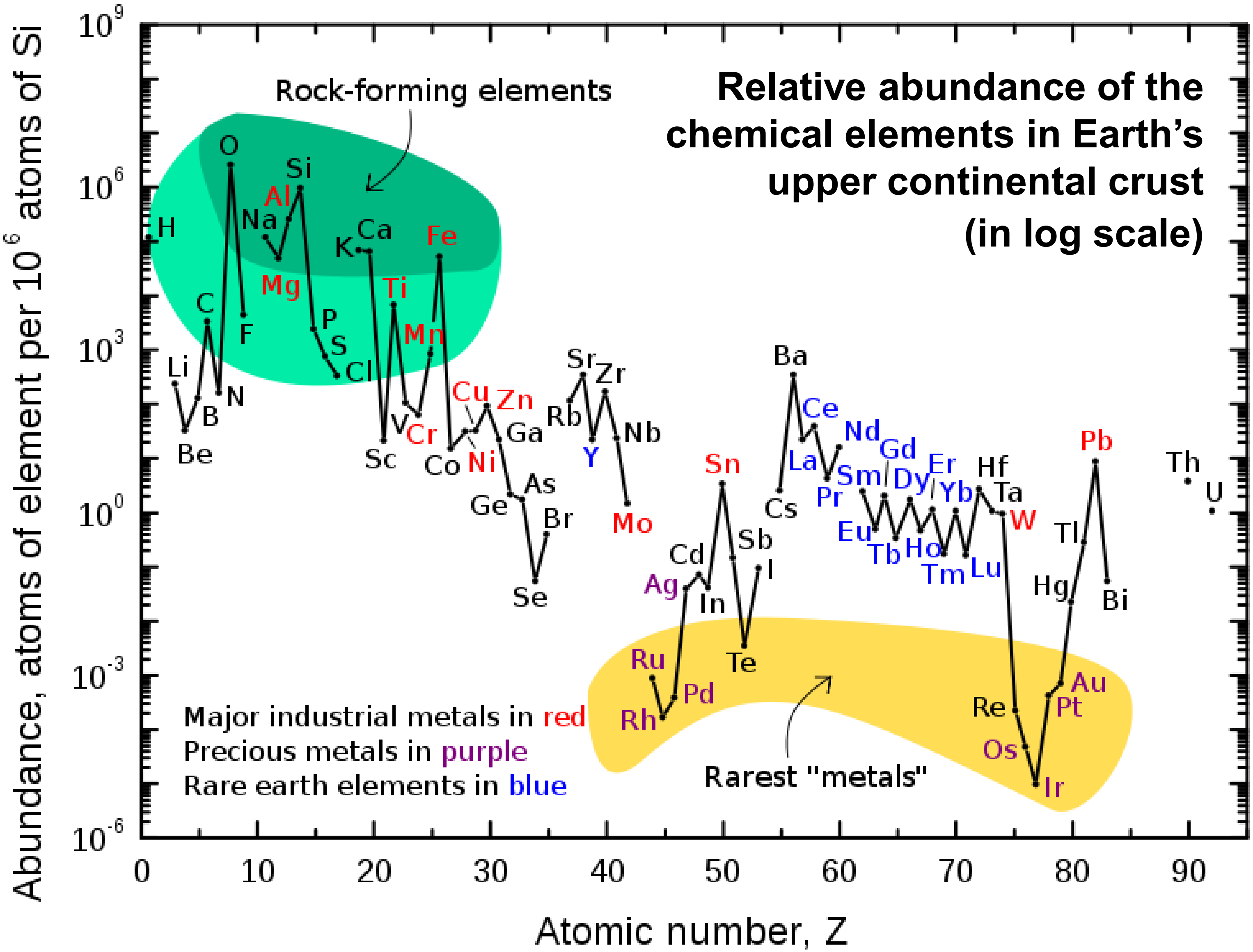

http://en.wikipedia.org/wiki/File:Elemental_abundances.svg

Higher Manganese Silicides (HMS), Mn_nSi_{2n-m} or $MnSi_{1.75}$

- **Novotony Chimney Ladder Phase**

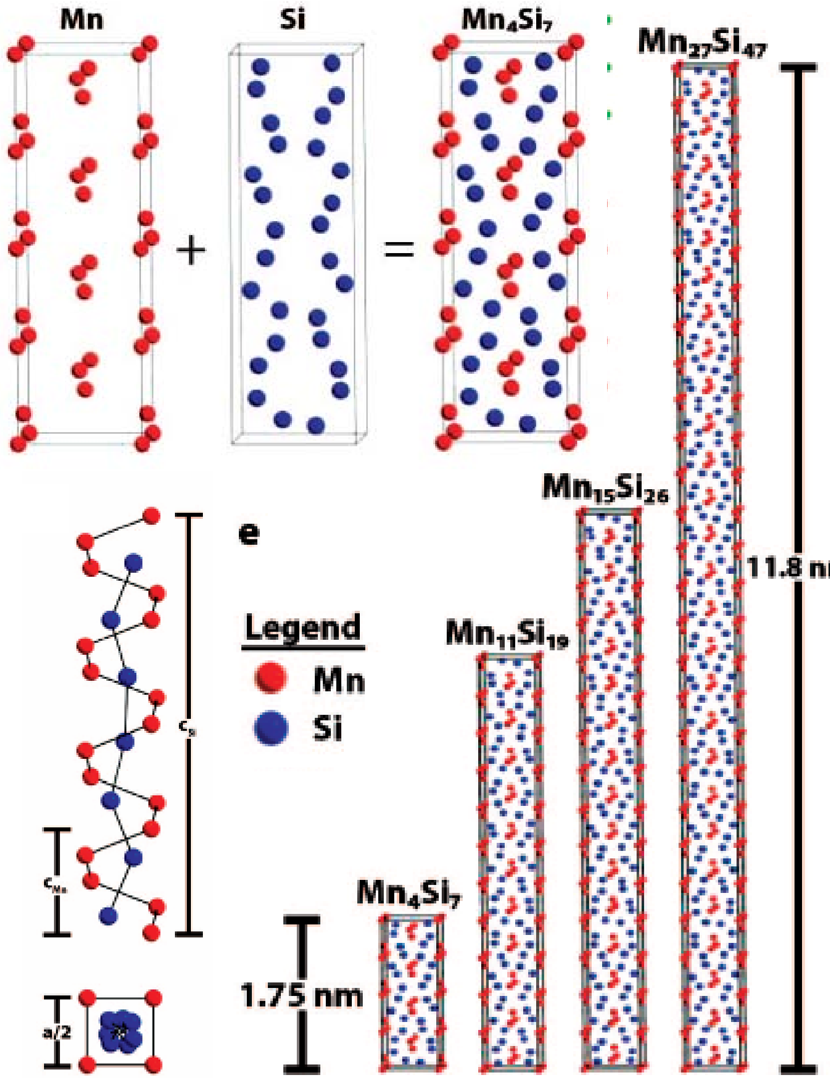

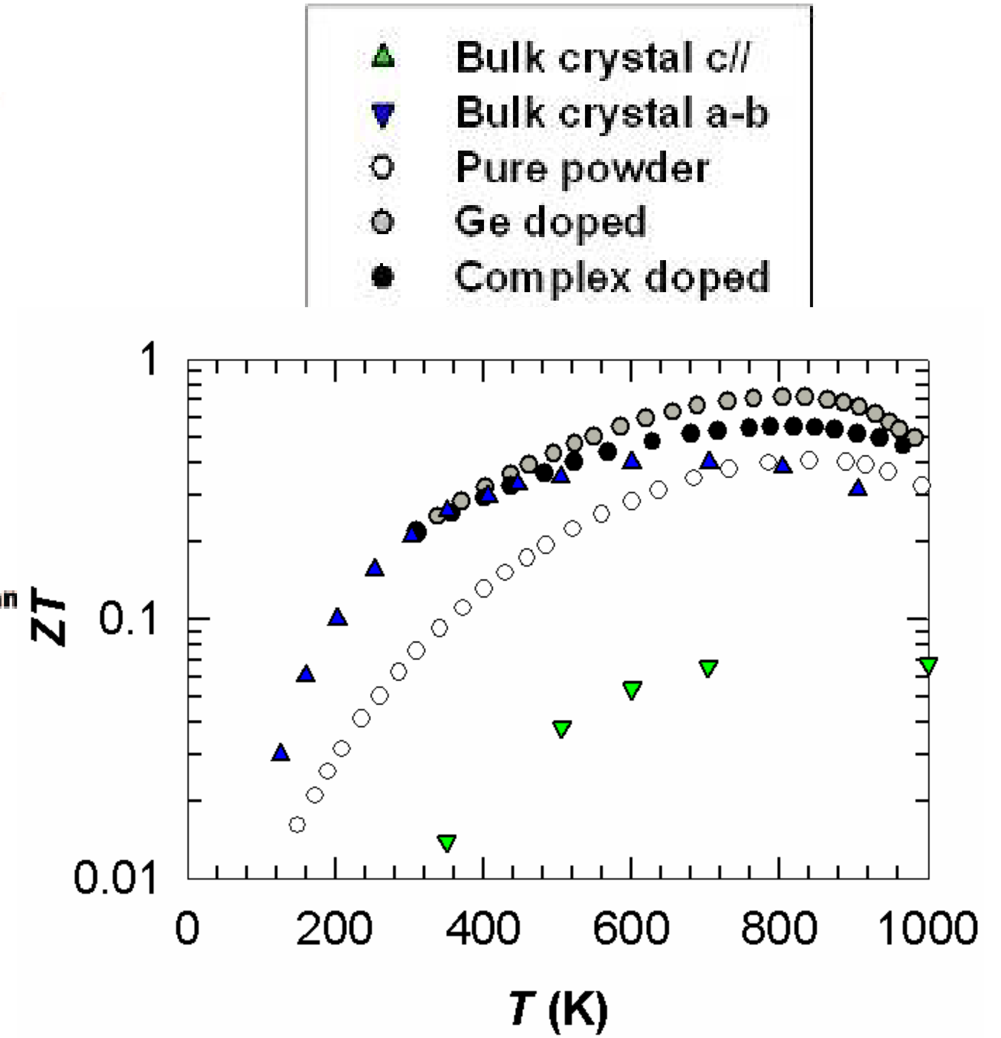

Data of Zaitsev et al., in *CRC Handbook of Thermoelectrics*, 1994, Ed. Rowe

Higgins & Jin, *JACS*, 130, 16086 (2008)

Phonon Transport in HMS

- Very long *c* gives small first Brillouin zone, long minimum wavelength.

- The low group velocity of numerous optical phonon modes and enhanced phonon-phonon scattering results in low $\kappa = 2\text{–}4$ W/m-K and *ZT* = 0.7 at 800 K in bulk $MnSi_{1.75}$.

- The low frequency acoustic phonons are not suppressed effectively by the complex structures.

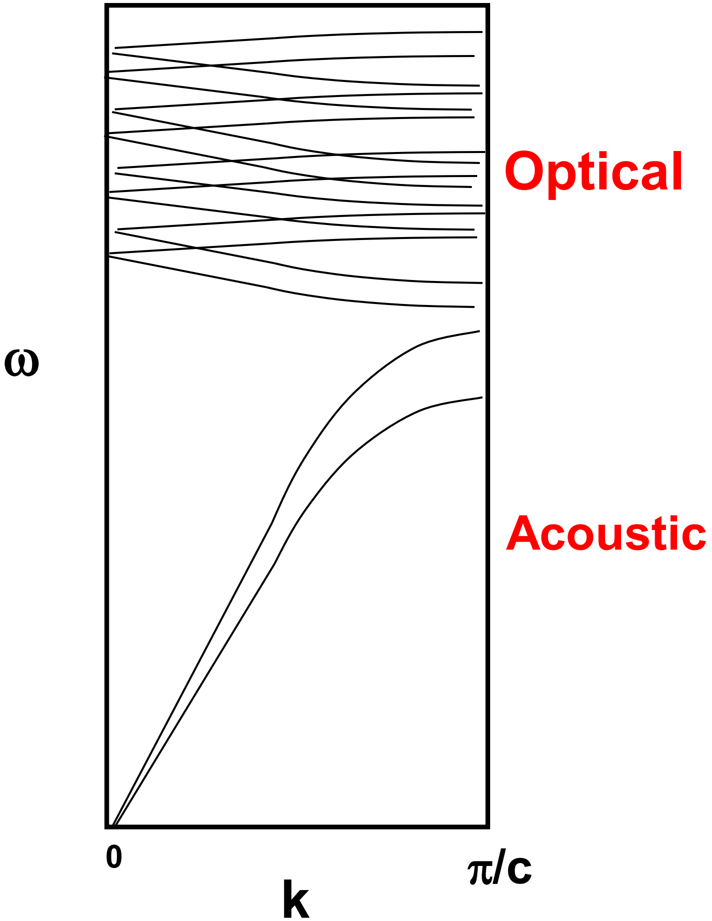

HMS Nanowires Synthesis and Characterization

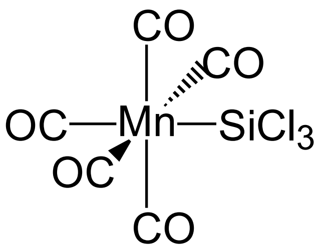

CVD

750 °C

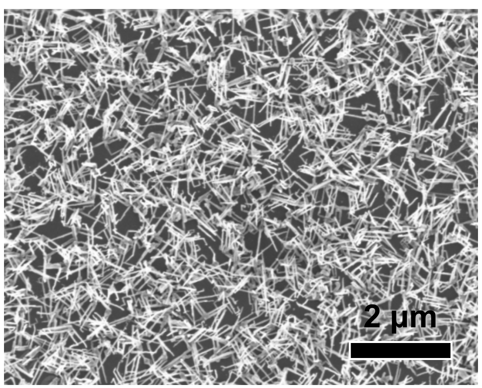

Zhou, Sczczech, Pettes, Moore, Jin, Shi, Nano Lett. **2007**, *7*, 1649.

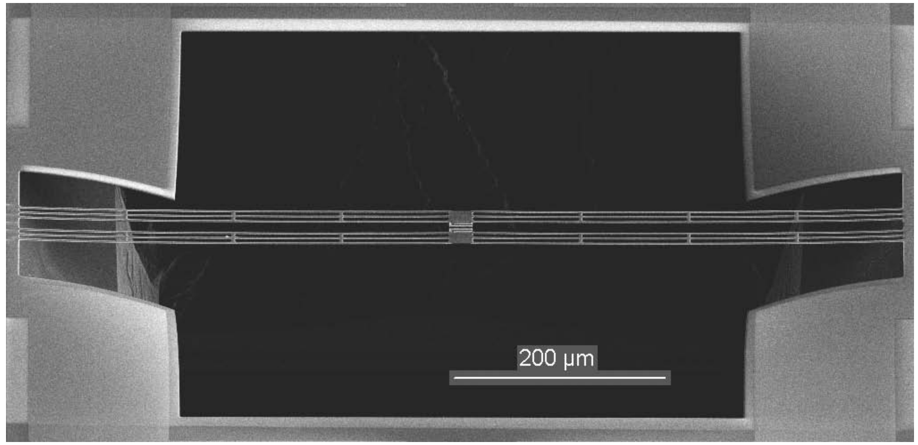

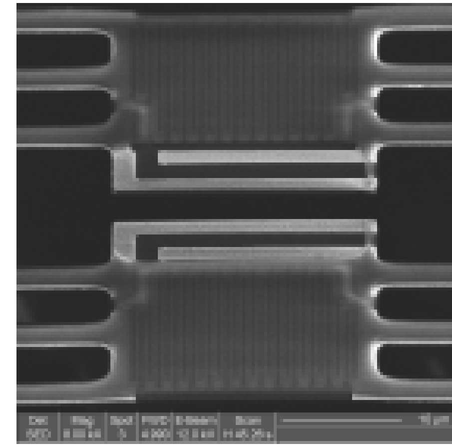

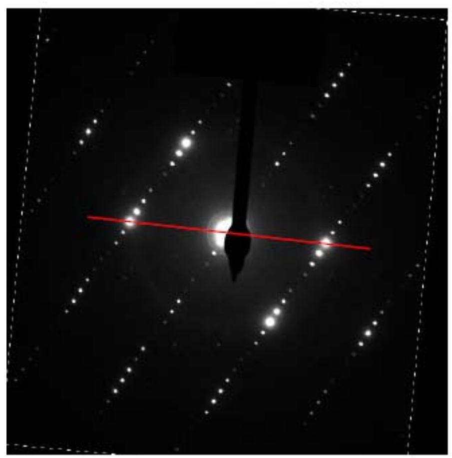

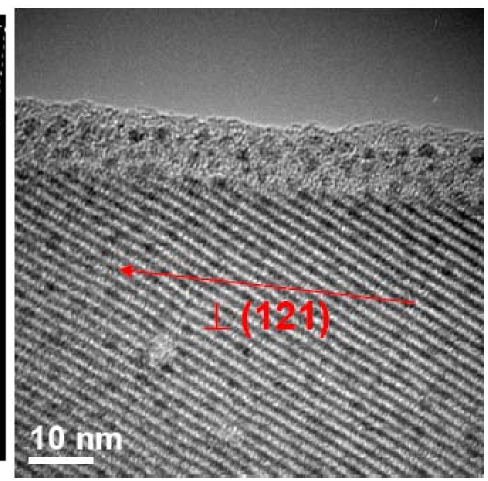

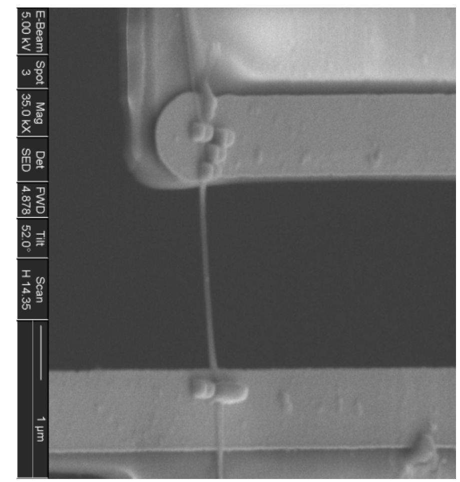

HMS NW synthesis: *Higgins & Jin JACS* **2008**, *130*, 16086.
Silicide NW review: *J. Mater. Chem.* **2010,** *20*, 223.

- Nanoribbon (NR) or NWs of $Mn_{39}Si_{68}$ or $Mn_{19}Si_{33}$
- c ≈ 17 nm
- Growth direction perpendicular to {121} planes, or 63^{o} from the c axis

Amorphous Thermal Conductivity in HMS NRs and NWs

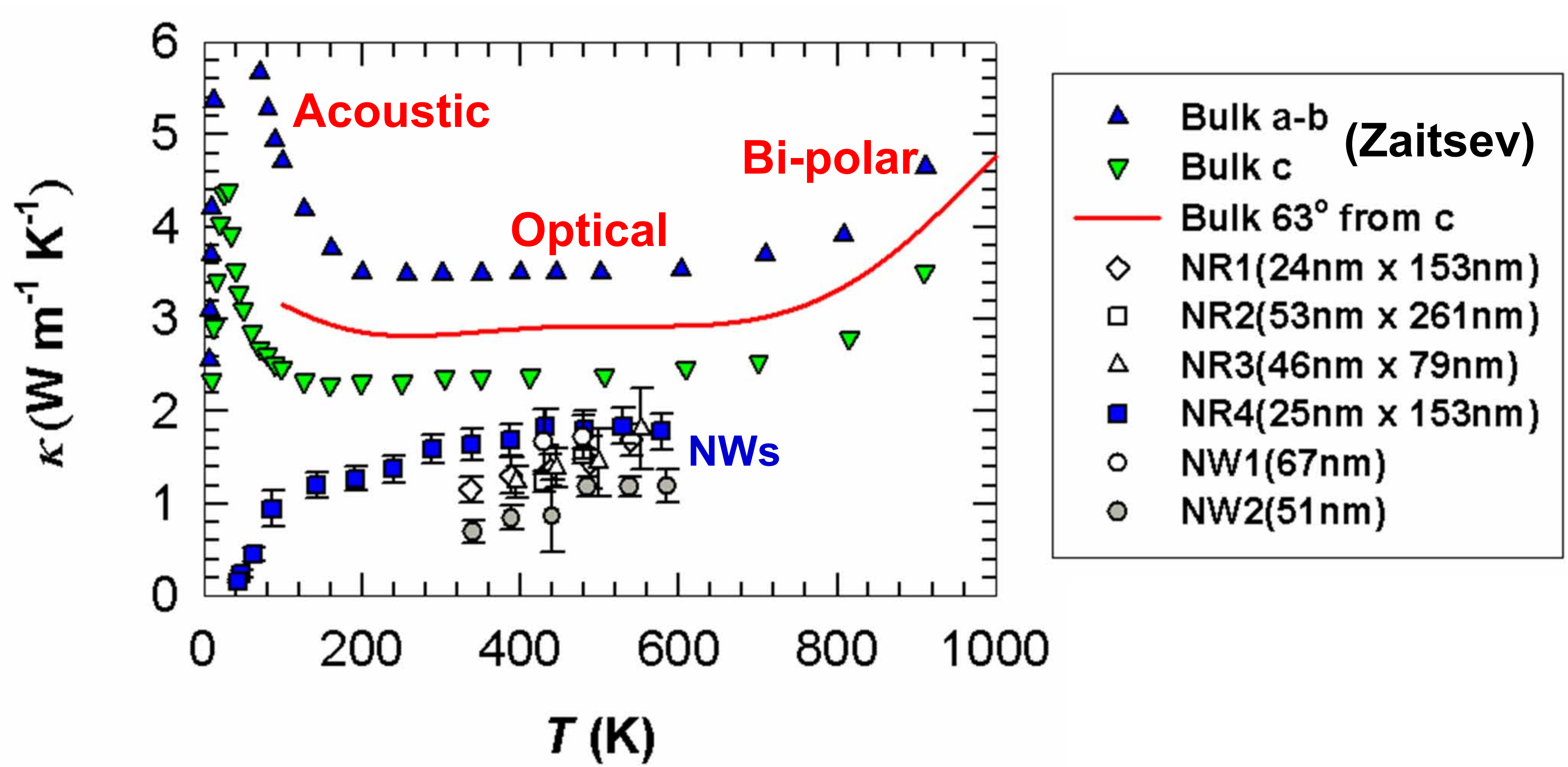

• Calculated amorphous thermal conductivity limit $\kappa_\alpha \approx 0.7$ W/m-K.

• The transition from the phonon-crystal behavior in bulk to amorphous thermal conductivity in the $MnSi_{1.75}$ nanostructures reveals effects of surface scattering, especially for long-wavelength phonons.

Size Effect on Electron Transport in $MnSi_{1.75}$ NWs

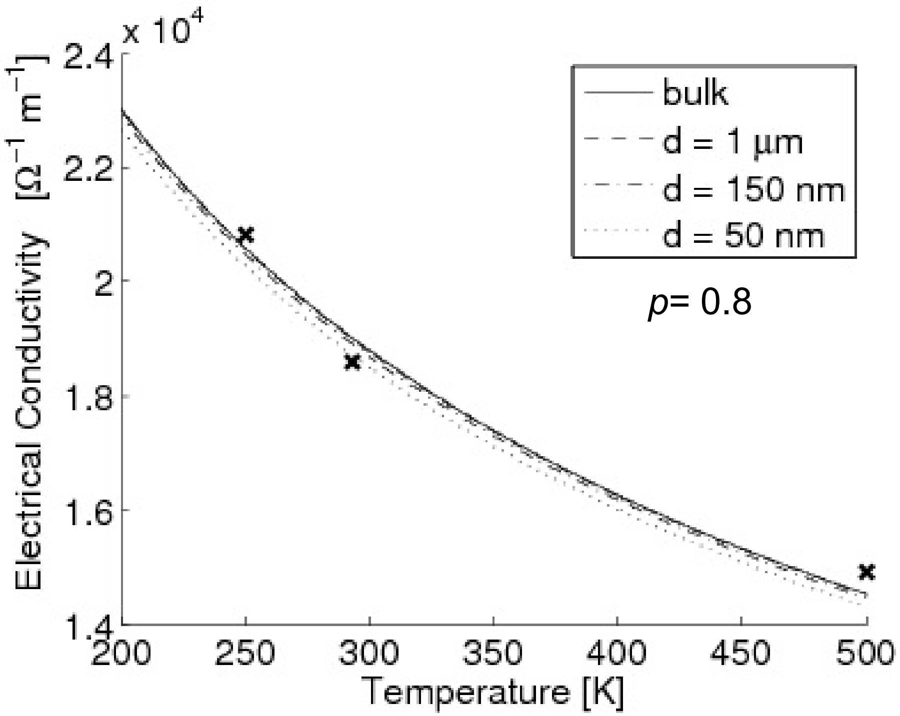

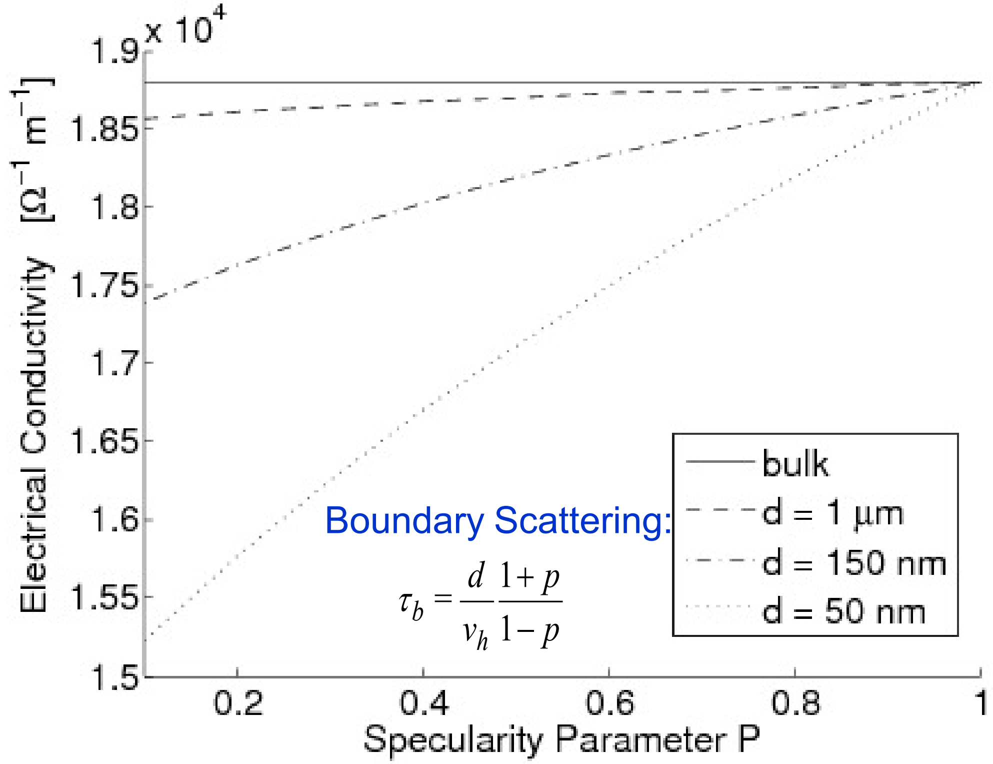

$$\sigma = \frac{q^2}{3\pi^2 m^*}\left(\frac{2k_B T m^*}{\hbar^2}\right)^{3/2}\int_0^\infty \frac{\tau x^{3/2} e^{x-\varsigma}}{\left(e^{x-\varsigma}+1\right)^2}dx$$

Relaxation Time: $$\frac{1}{\tau} = \frac{1}{\tau_{e-p}} + \frac{1}{\tau_{imp}} + \frac{1}{\tau_b}$$

Electron-Phonon Scattering:

$$\tau_{e-p} = \frac{h^4 v^2 \rho}{\left(8\pi^2\right)^{3/2} k_B T \Delta^2}\,\frac{E^{-1/2}}{m^{*3/2}}$$

Impurity Scattering:

$$\tau_{imp} = \left(\frac{2\mathrm{m}^*}{\pi^3}\right)^{1/2} \frac{8\varepsilon_0 E^{3/2}}{n_i q^4 \log\left\{1+\left(3\varepsilon_0 k_B T / q^2 n_i^{1/3}\right)^2\right\}}$$

Parameter	Reference	Parameter	Reference
$m_h^* = 15\ m_e$	[1]	$E_g = .84$ eV	[7]
$n = 2\times10^{27}\ \mathrm{m}^{-3}$	[1]	$\Delta = 8eV$	[6]
$\mathrm{n}_{imp} = 2.24\times10^{24}\ \mathrm{m}^{-3}$	fitted	$\rho = 5000\ \mathrm{kg/m}^3$	[10]
$v_s = 10^5$ m/s	fitted		

Bulk HMS Synthesis via Two-step Solid-State Reaction

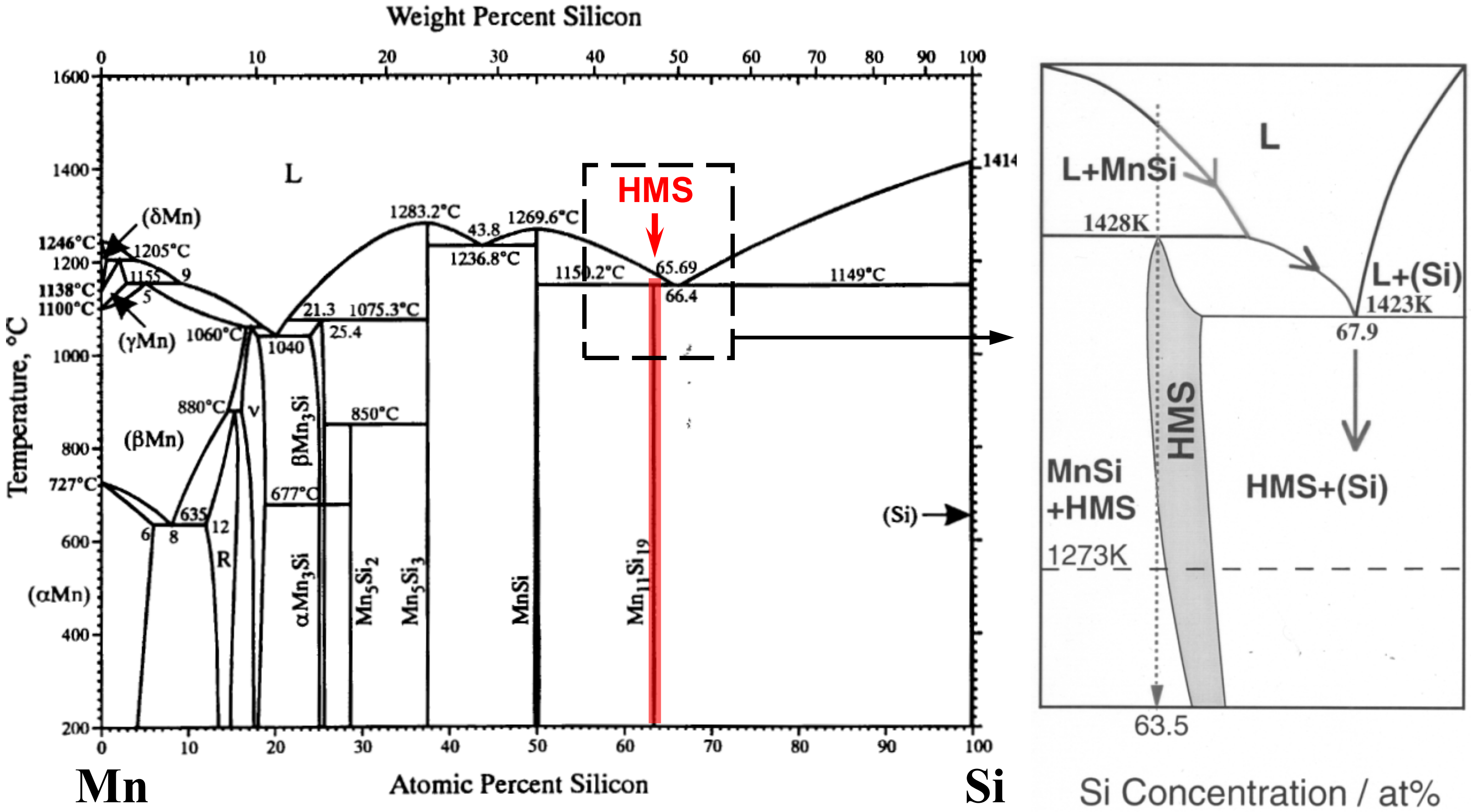

Mn + Si —Ball milling, 1 h→ Mn, Si mixture —Sealed in a tube, 973 k,48 h→ ingot —Grinding→ powder —Ball milling, 1 h→ mixture —Sealed in a tube, 1473 k,48 h→ HMS

XRD and Microstructures of Bulk HMS

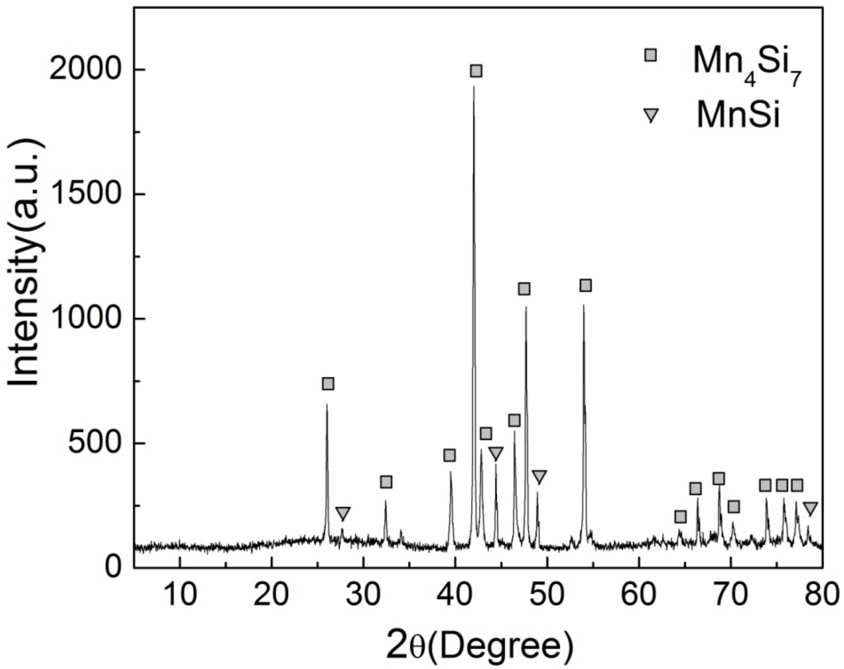

SEMs of HMS sample surface after polishing and 60-s selective etching of MnSi in $HF:HNO_3:H_2O$=1:6:13

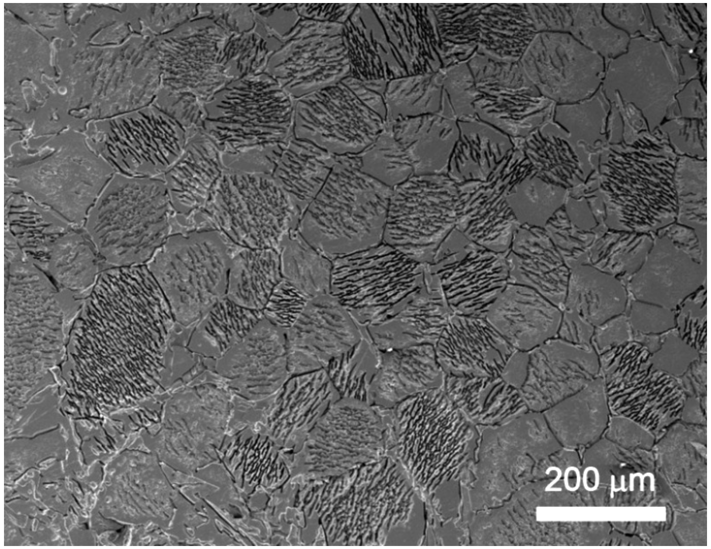

MnSi layers etched away

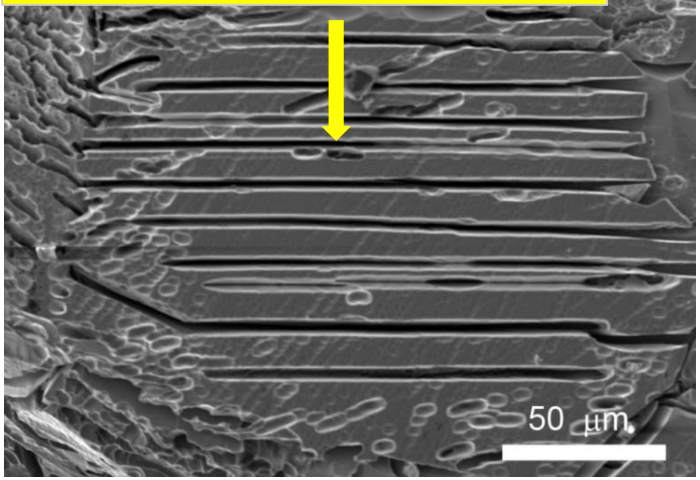

MnSi particles etched away

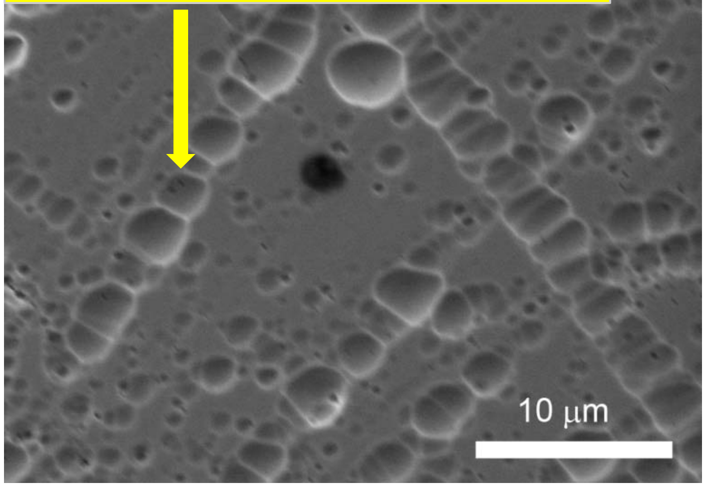

TE Properties of Bulk Undoped HMS

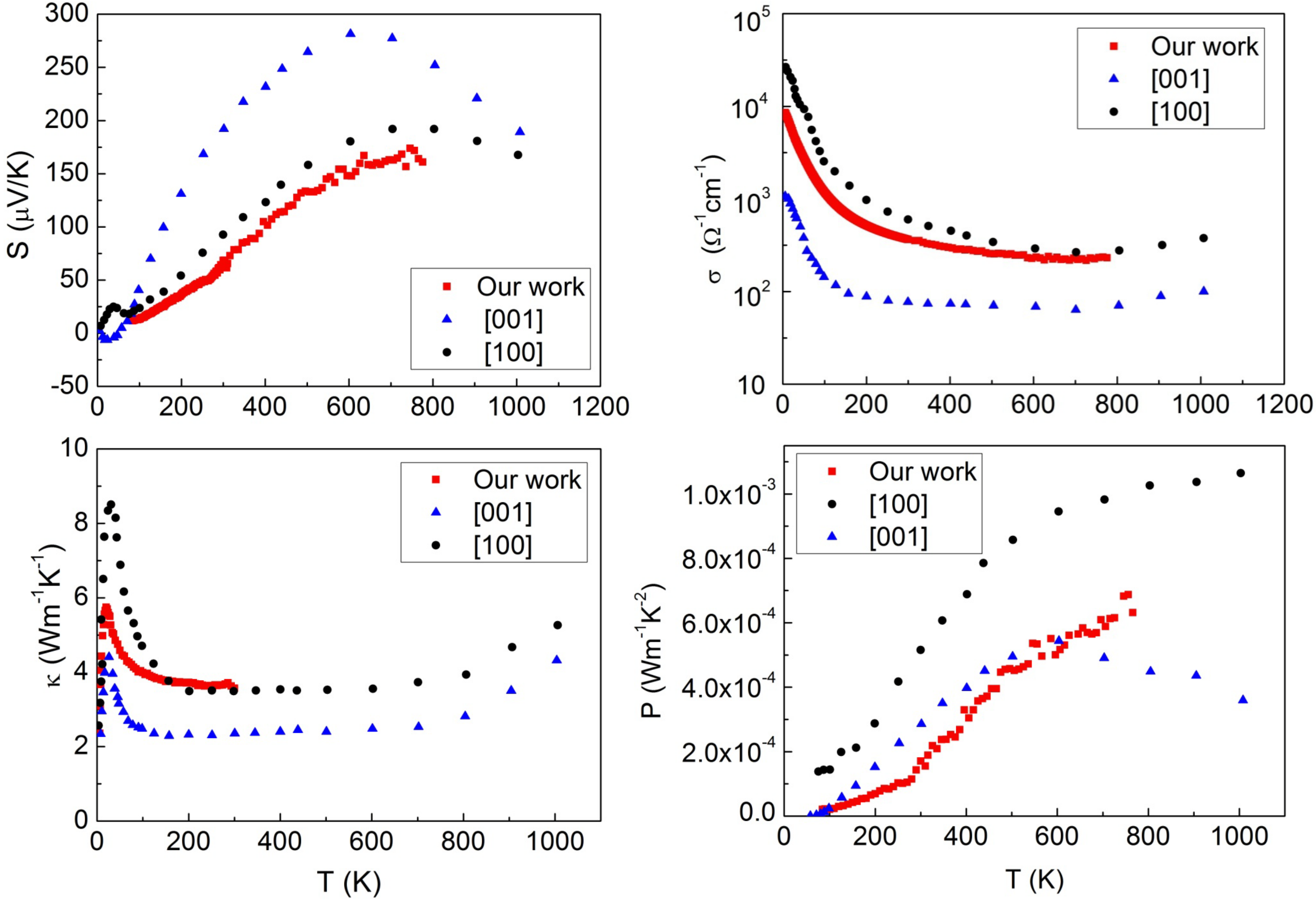

Literature data from Zaitsev et al, in *CRC Handbook of Thermoelectrics*, 1994, Ed. Rowe

Future Directions in HMS Materials Research

- **Turn MnSi micro- layers and particles in HMS into nanoparticle inclusion to scatter long wavelength phonons**
- **Bulk nanostructured HMS via conversion (see next slide)**
- **Ball milling / solution synthesis of HMS nanoparticles for making bulk nanocomposites**
- **To tune the *ZT* peak position via position-dependant doping**

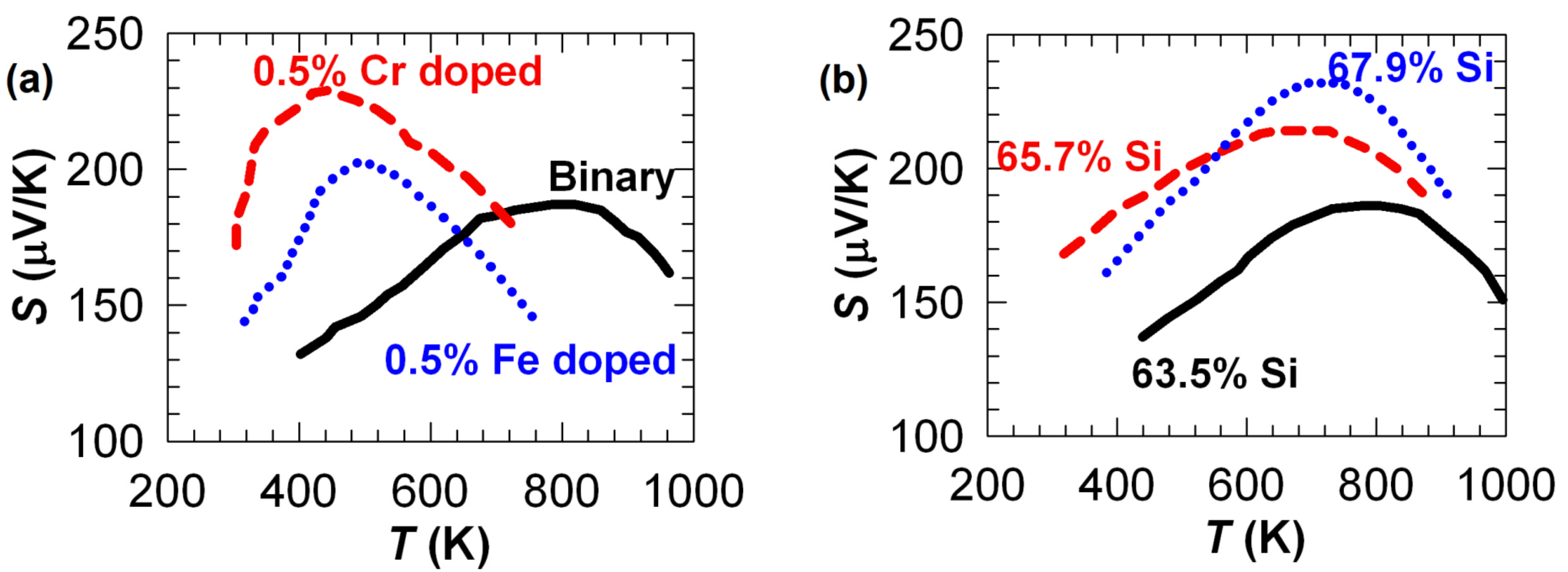

K. Kakubo, Y. Kimura, and Y. Mishima, "Microstructures and thermoelectric power of the higher manganese silicide alloys," *Mat. Res. Soc. Symp. Proc.* , vol. 646, p. N2.9.1 (2001).

Converting Diatomaceous Earth into Bulk Nanostructured Silicides

Szczech & Jin *J. Solid State Chem.* 2008, *181*, 1565.

Silica

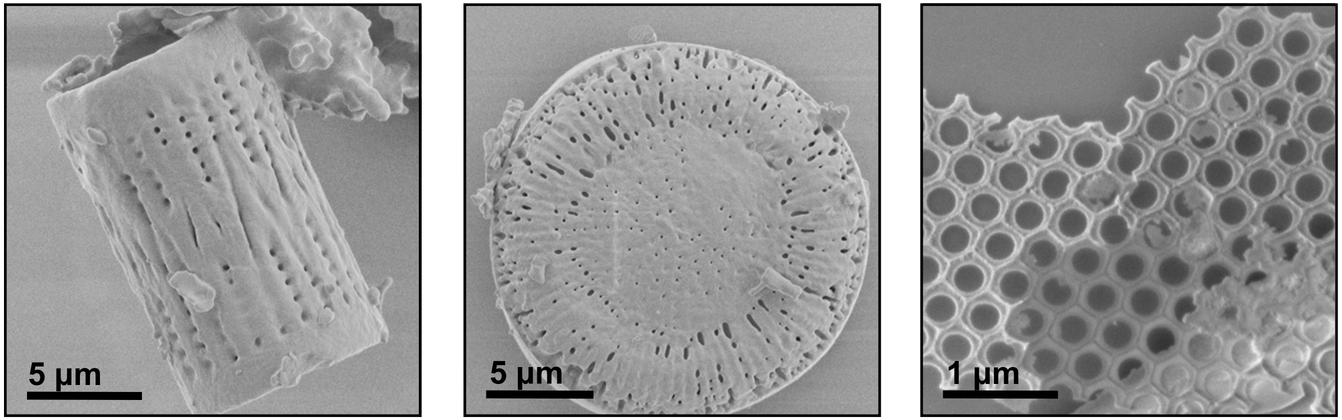

SiO_2 *(s)* + 2 Mg *(g)* → Si *(s)* + 2 MgO *(s)*
Si *(s)* + 2 Mg *(g)* → Mg_2Si *(s)*

Mg_2Si/MgO composite with nanoscale grains

Mg_2Si
(silicon)

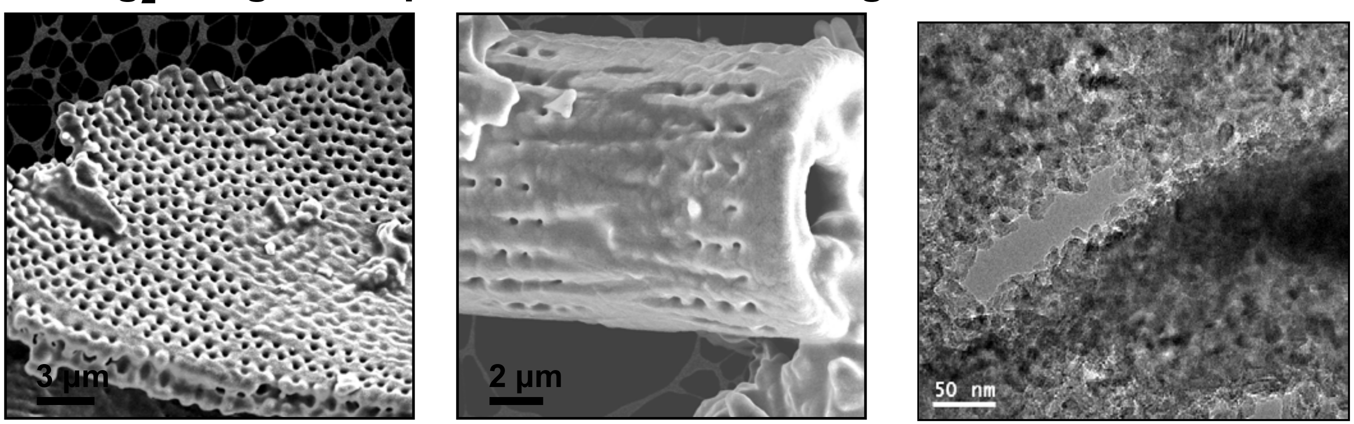

Future work: Expand to doped $MnSi_{1.75}$ and $Mg_2Si_{1-x}Sn_x$

Improved thermoelectric properties of $Mg_2Si_xGe_ySn_{1-x-y}$ nanoparticle-in-alloy materials

S. Wang[1,a)] and N. Mingo[2]

APPLIED PHYSICS LETTERS **94**, 203109 (2009)

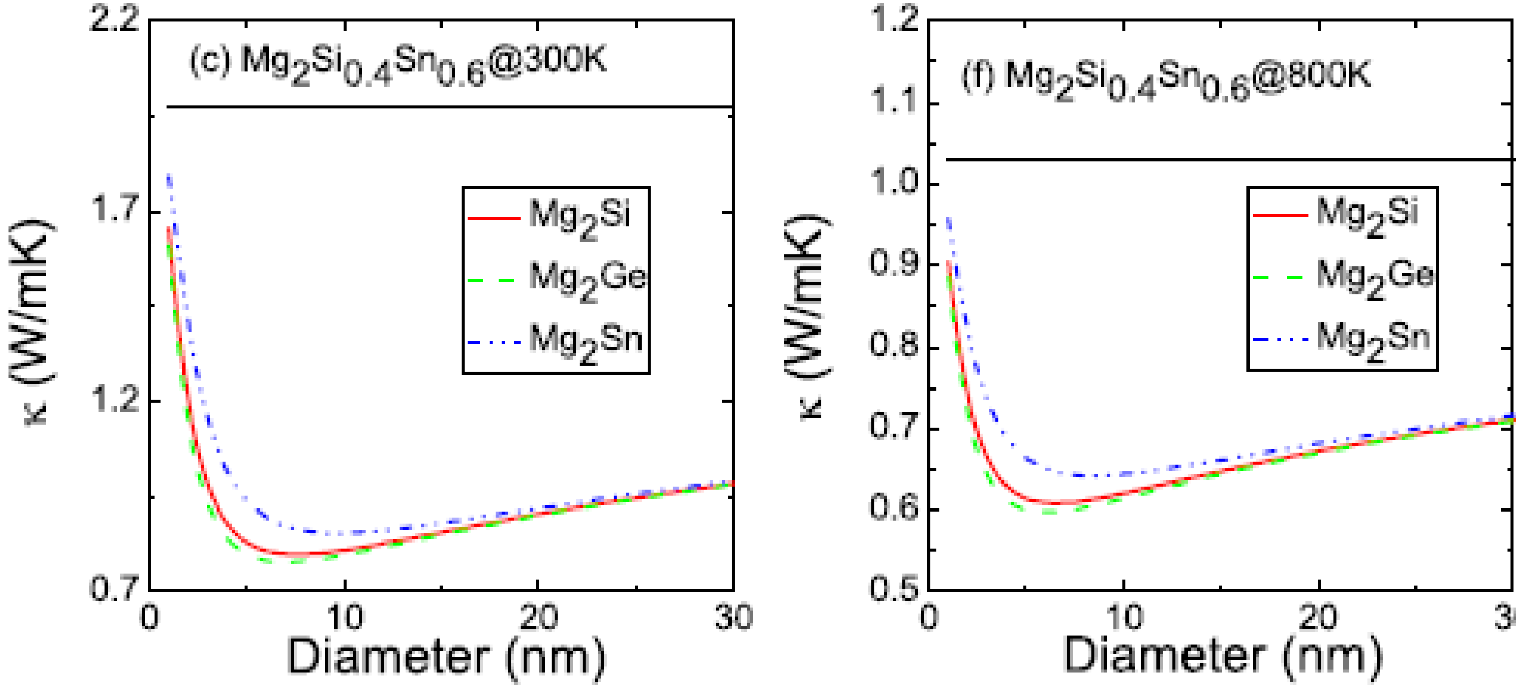

FIG. 1. (Color online) Calculated thermal conductivities (κ) of different $Mg_2Si_xGe_ySn_{1-x-y}$ NEAT materials as a function of particle diameters at 300 K and 800 K with 3.4% nanoparticle volume fraction. The horizontal lines denote calculated κ of [(a) and (d)] $Mg_2Si_{0.4}Ge_{0.6}$, [(b) and (e)] $Mg_2Ge_{0.4}Sn_{0.6}$, [(c) and (f)] and $Mg_2Si_{0.4}Sn_{0.6}$ matrices for comparison.

Implementation in a 6.7 liter Cummins Diesel Engine

Exhaust after-treatment (DOC/DPF)

Engine

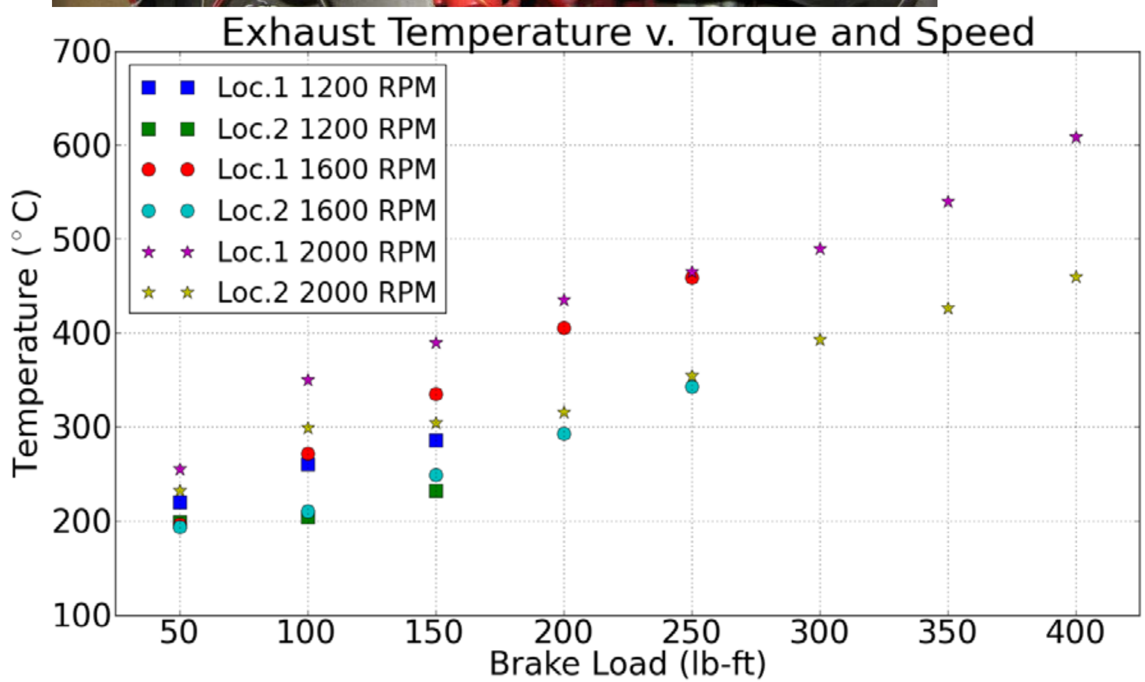

Preliminary Thermodynamic Systems Model

- Primary constraints: maintain temperature of 250°C into exhaust after-treatment system, maintain acceptable pressure drops throughout exhaust system.
- **Assumptions**: TE heat exchanger is able to extract all available heat subject to temperature constraints and with cold side temperature of 25°C.
- Model has yet to account for spatial variation of TE properties along TE module

$$\eta_{TE,max} = \frac{\Delta T}{T_h} \frac{\sqrt{1+ZT}-1}{\sqrt{1+ZT}+T_c/T_h}$$

$$\eta_{sys} = \frac{\eta_{TE}\dot{Q}_h - \dot{W}_{pumping}}{\dot{m}\psi}$$

Configuration 5

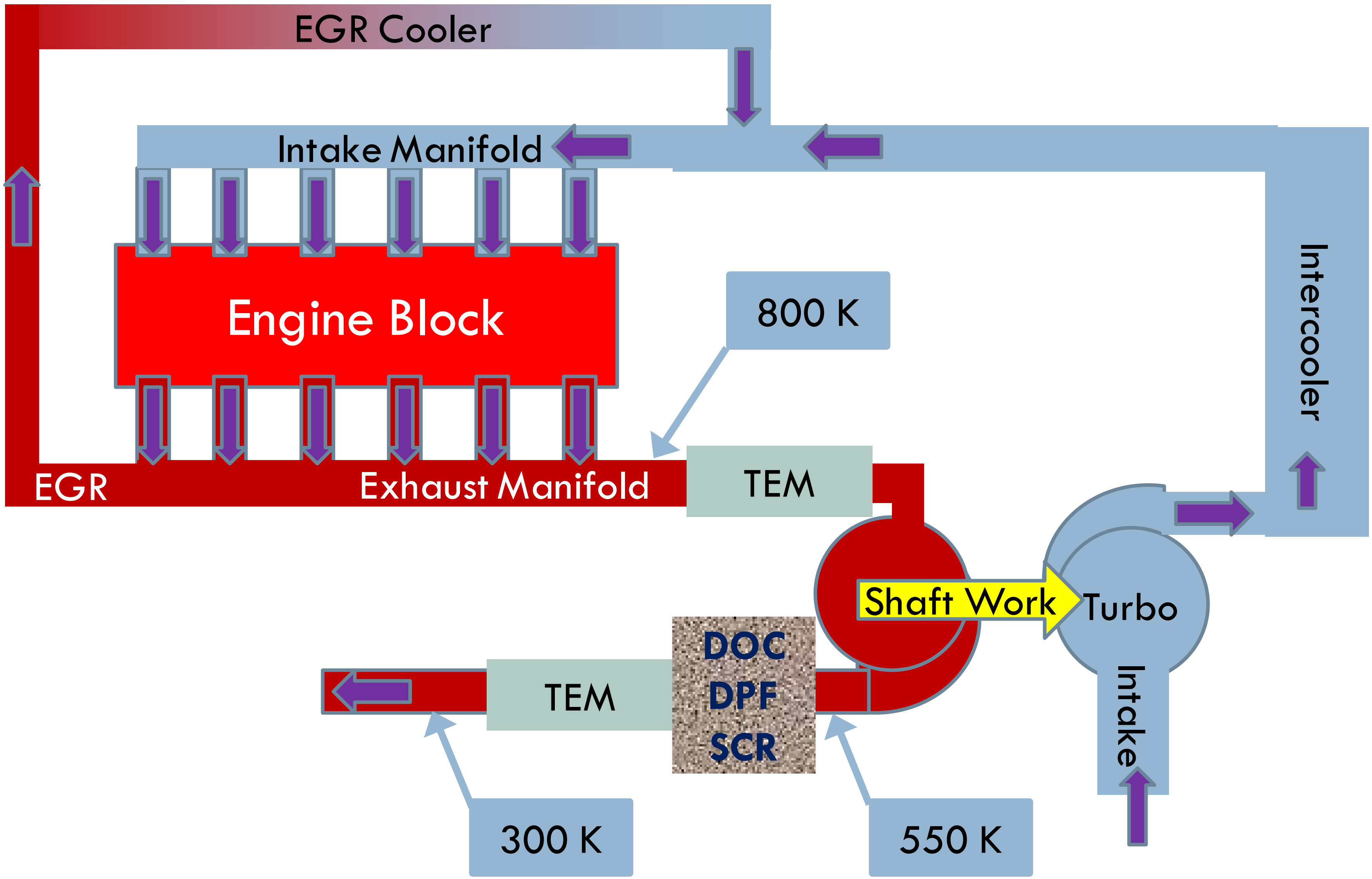

Maximum Possible Thermoelectric Power

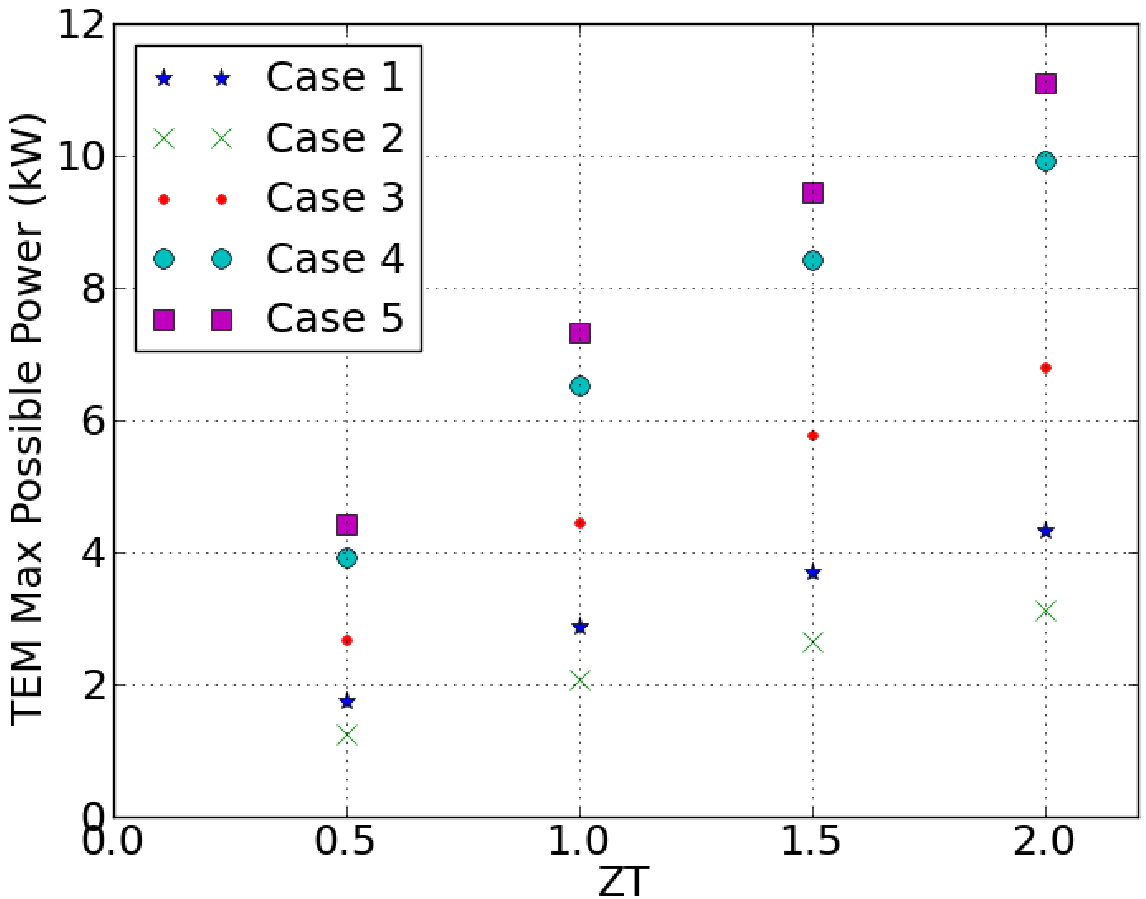

- **RPM = 2000**
- **Brake Torque = 300 lb-ft**
- **Charge flow rate = 7.8 kg/min**
- **Exhaust port temperature = 800 K**
- **Engine exhaust availability = 81.1 kW**

Case 1: single TEM > turbo > after-treatment

Case 2: turbo > single TEM > after-treatment

Case 3: turbo > after-treatment > single TEM

Case 4: turbo > TEM > after-treatment > TEM

Case 5: TEM > turbo > after-treatment > TEM

Summary

• In nanostructured complex $MnSi_{1.75}$, the contributions to κ from high-frequency phonons and low-frequency phonons are suppressed by the complex structure and interface scattering, respectively, to obtain glass-like thermal conductivity.

• While it remains to be verified, the large hole effective mass and large carrier concentration can potentially lead to effective screening of surface states/scattering, so that potentially the power factor is reduced as much as κ_l suppression in $MnSi_{1.75}$ nanostructures, similar to our prior finding on $CrSi_2$ nanowires (Nano Lett 2007, 7, 1649).

• Bulk $MnSi_{1.75}$ and $Mg_2Si_{1-x}Sn_x$ with nano-grains or nanoparticle inclusion are being synthesized via both solid state reaction and chemical conversion from diatomaceous earth.

• Preliminary exhaust temperature measurements and thermodynamic modeling results suggest that two thermoelectric modules, one upstream of the turbo and the other downstream of the exhaust after-treatment equipment, would considerably increase the power output. Additional enhancement is expected by extracting the EGR flow downstream rather than upstream of the 1st stage module.

Configuration 1

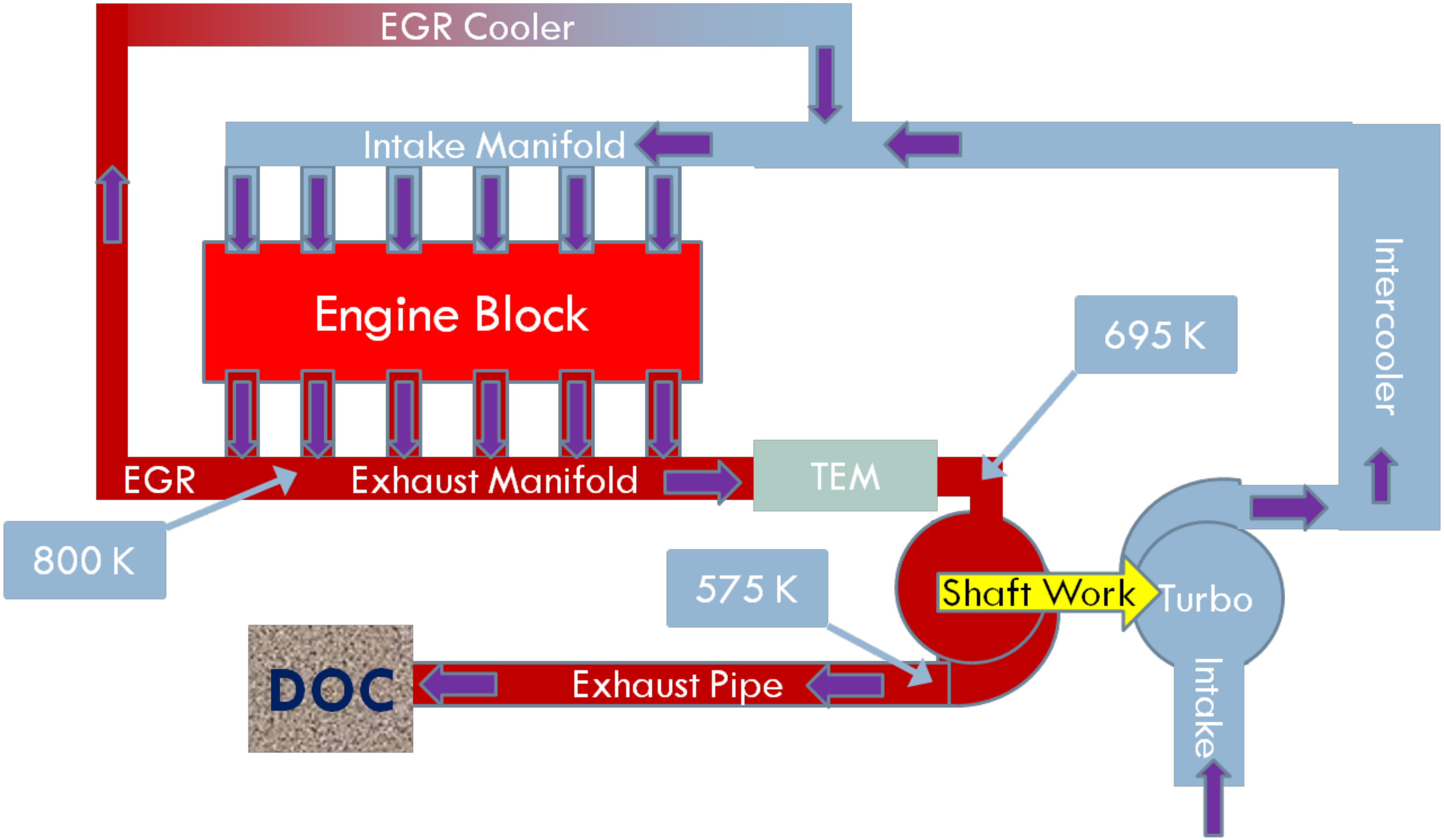

Configuration 2

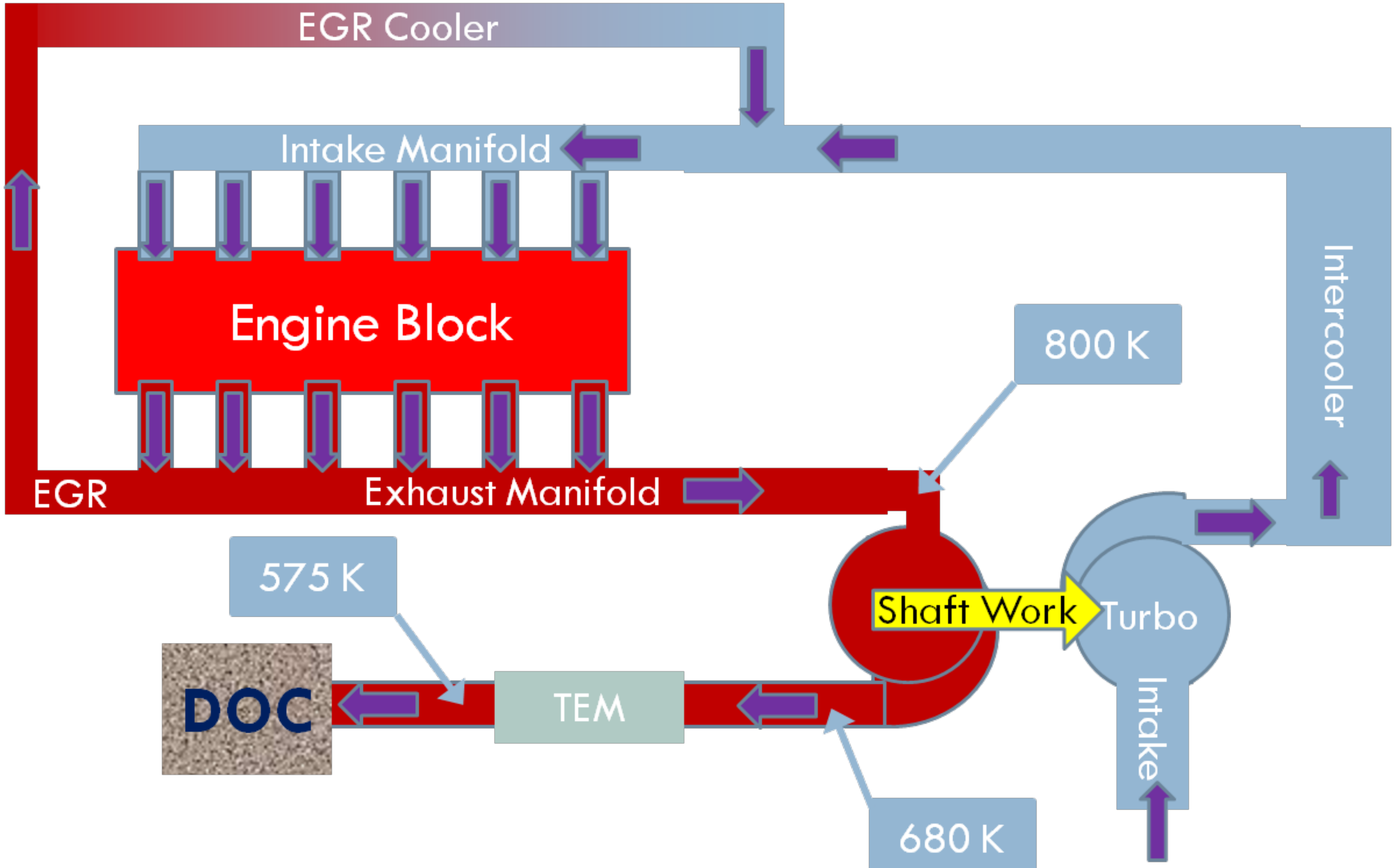

Configuration 3

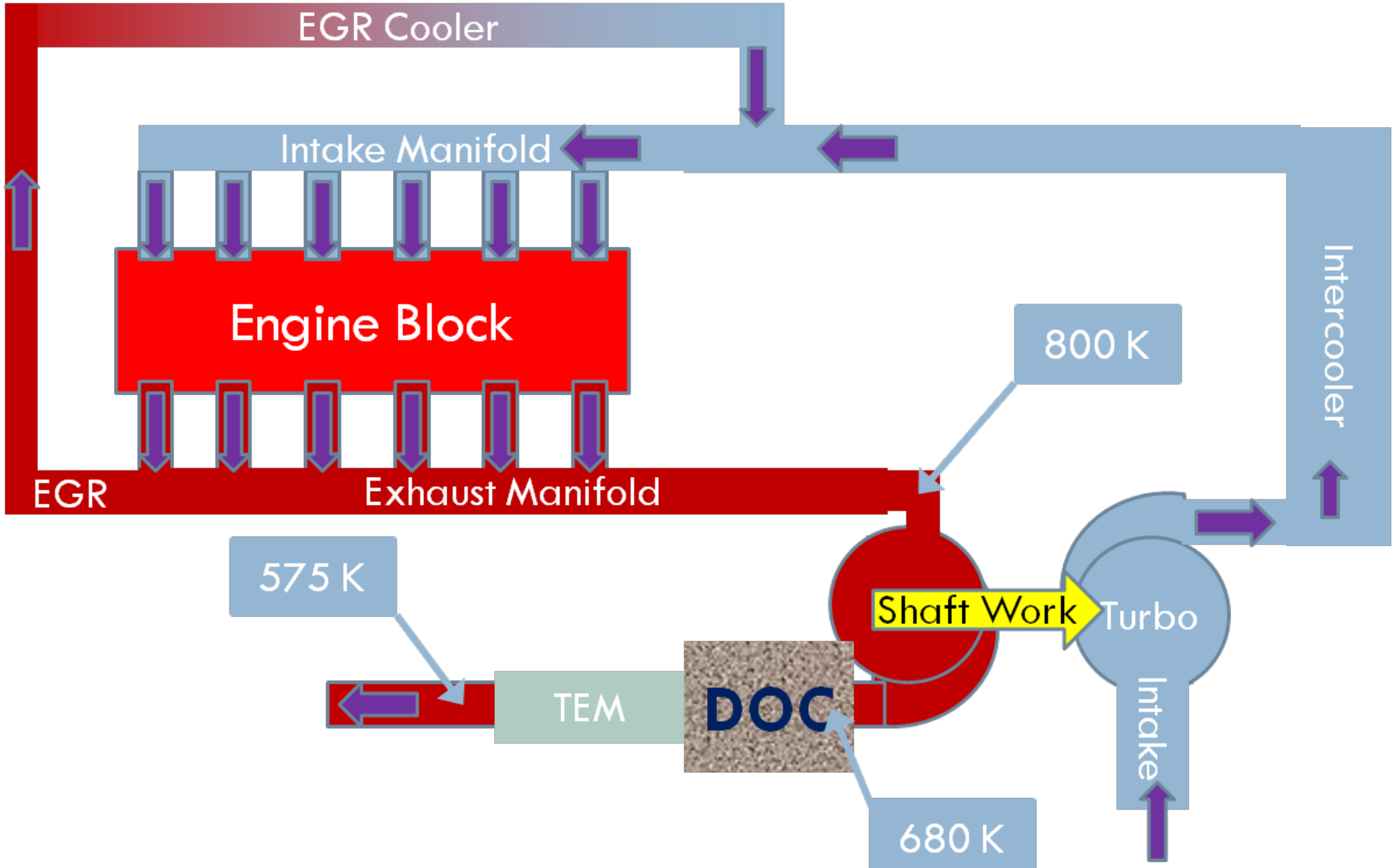

Configuration 4

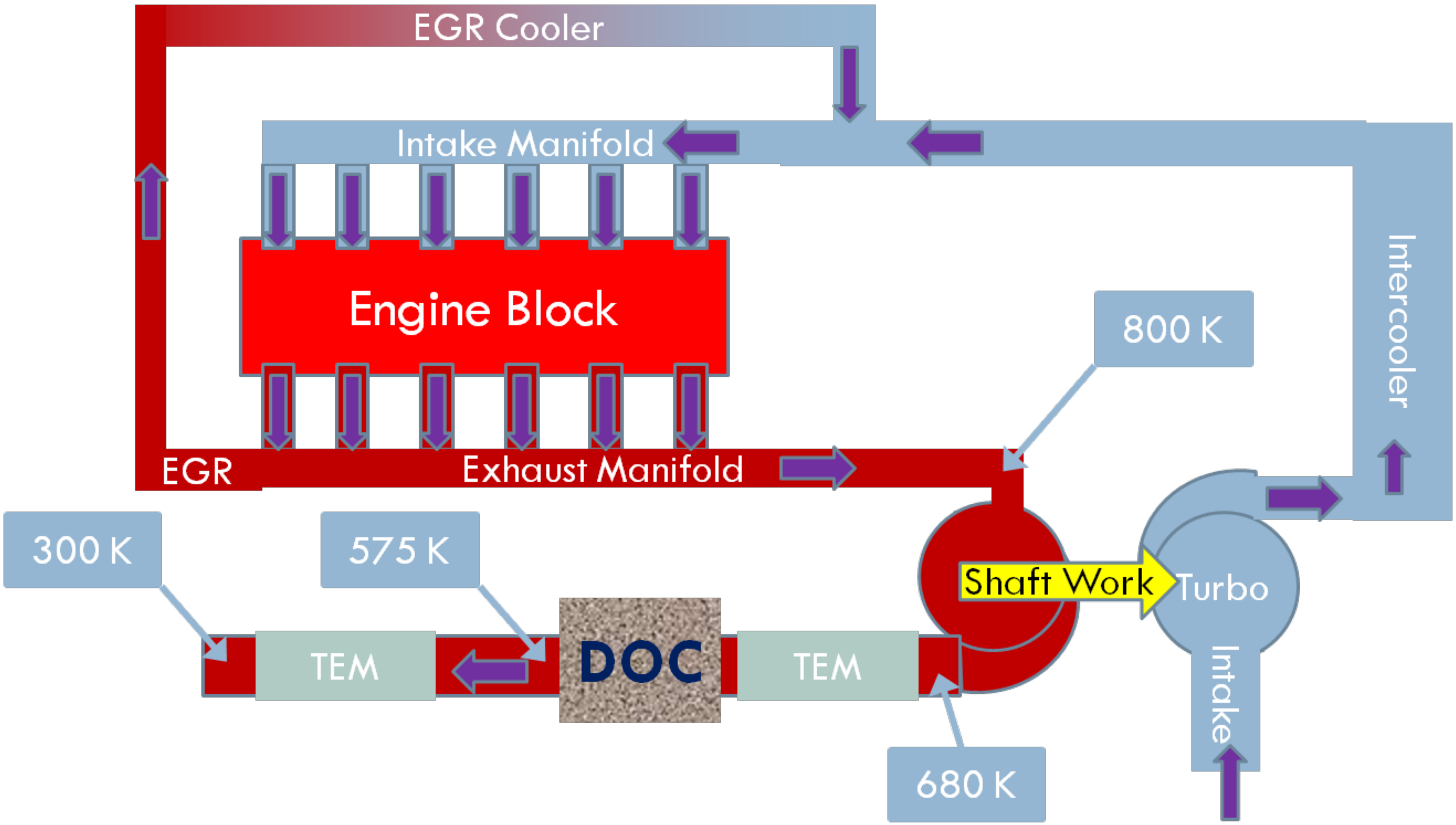

Implementation in a 6.7 liter Cummins Diesel Engine

- **Engine data currently being gathered as inputs to models.**
- **Temperatures**: exhaust port and downstream of turbine
- **Pressures**: exhaust manifold, boost pressure, pressure between turbine and DOC/DPF
- **Flow rates**: air, fuel, and EGR

Systems Modeling

- Two computer models currently being developed
  - **Thermodynamic systems model** to optimize thermoelectric device locations in engine exhaust
  - **Heat Transfer model** for improving TE module performance
  - Both to be integrated as one model and to account for transient exhaust conditions
- Components include:
  - TE Module(s)
  - Turbocharger
  - Exhaust aftertreatment system
  - EGR cooler